Journal of Alloys and Compounds 480 (2009) 416–421

Contents lists available at ScienceDirect

Journal of Alloys and Compounds

journal homepage: www.elsevier.com/locate/jallcom

Effects and on-line prediction of electromagnetic stirring on microstructure refinement of the 319 Al–Si hypoeutectic alloy

F.C. Robles Hernández [a,*], J.H. Sokolowski [b]

[a] University of Houston, 304 A Technology Building, Mechanical Engineering Technology, Houston, TX 77204-4020, United States
[b] Light Metals Casting Technology (LMCT) Group, Room 212A, Essex Hall, 401 Sunset Avenue, Windsor, ON, Canada, N9B 3P4

ARTICLE INFO

Article history:
Received 14 January 2009
Received in revised form 21 February 2009
Accepted 23 February 2009
Available online 9 March 2009

Keywords:
Aluminum alloys
Electromagnetic stirring
Thermal analysis
Melt treatments
Grain size

ABSTRACT

In this paper are presented the results of the electromagnetic treatment used to refine 319 aluminum alloy in semi-solid state. The severity of the treatment is controlled by varying the intensity of the electromagnetic field (using different AC current), which results in the different levels of microstructure modification. In this research is found that the main microstructure characteristics that are sensitive to electromagnetic stirring modification are grain size, dendrite size and a Cu phase. The electromagnetically stirred material is transformed from a dendritic structure into quasi-cellular one with a grain size refinement of up to 600%. Conversely, the silicon present in the Al–Si eutectic did not present significant modification. The results of image and thermal analysis are in good agreement allowing to propose a mathematical approach that can be used for on-line prediction of the level of microstructure modification of the ES treated melt.

© 2009 Published by Elsevier B.V.

1. Introduction

The replacement of high density materials, such as cast iron and steel, by light metals alloys are of interest in the last few decades, in particular for the automotive and the aerospace industries [1]. For this and other reasons the development of novel manufacturing technologies is crucial, these new developments have as a main objective the improvement in mechanical properties. This in turn may result in weight reduction, which have a direct impact in fuel efficiency, thus emissions reduction. Several research publications indicate that electromagnetic stirring (ES), mechanical stirring, ultrasonic vibration, electromagnetic stirring and vibration and semisolid metal forming techniques have been successfully used. These methods are commonly applied in semi-solid state having positive effects on mechanical properties of structural, service and mechanical characteristics of ferrous and non-ferrous alloys [2–8].

The previously mentioned processes are commonly applied in semi-solid state that is mainly due their effectiveness in refining early forming dendrites. Additionally, this improves the fluidity of the melt allowing lower casting temperatures. Due to the high fluidity of the ES treated melts, the casting/super heat temperature can be reduced to temperatures as low as liquidus. Based in common casting practices this can represent a temperature reduction of approximately 150–200 °C, which can reduce cost. Further advantages of semi-solid alloy processing include reduction in the size of inclusions, micro/macro-porosity and segregation that may improve mechanical properties [2–8]. Nowadays, some automotive components (e.g. brakes, suspension component, etc.) are manufactured using electromagnetic stirring, rheocasting, thixocasting and combined methods [7,9]. For some Al based alloys the effect of electromagnetic treatment can be further enhanced with chemical modification (like Sr, Na, P, etc.) [10,11]. In the literature has been reported that ultrasonic vibration can lead to the following improvements: 15% in ultimate tensile strength and 50–400% in elongation [9].

In the present paper are presented the results of feasibility studies of the semi-solid electromagnetic treatment applied to commercial 319 alloy in semi-solid state. The research presented herein is characterized by means of microstructure and thermal analysis. A new concept of using thermal analysis is presented as a unique approach to monitor the structure refinement for the Al–Si 319 alloy in as-cast (unmodified) and ES treated conditions. The results of thermal analysis are used to develop a simple mathematical model that can be used to predict microstructure refinement and phase modification of electromagnetically treated 319 alloy.

2. Experimental procedure

Ingots of 12 kg of commercial 319 alloy were melted in an electric resistance furnace and held at 750 ± 10 °C (approximately 150 °C above liquidus) during the experiments. The chemical composition of the 319 alloy is given in Table 1. The melt is degassed using a FOSECO Mobile Degassing Unit by blowing Ar gas at a rate of

* Corresponding author. Tel.: +1 713 743 8231.
E-mail address: fcrobles@central.uh.edu (F.C. Robles Hernández).

0925-8388/$ – see front matter © 2009 Published by Elsevier B.V.
doi:10.1016/j.jallcom.2009.02.109

Table 1
Chemical composition for the investigated 319 alloy (wt%).

Alloy	Al	Si	Cu	Ni	Fe	Mg	Zn	Sr (ppm)
319	Bal.	7.55	3.45	0.008	0.40	0.25	0.009	6

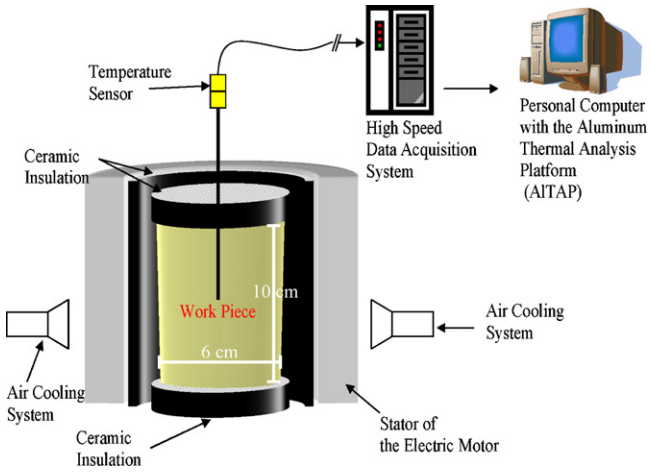

Fig. 1. Schematic drawing of the ES workstation used for 319 alloy melt treatments.

20 Standard Cubic Feet per Hour (0.57 m^3/h) through a graphite impeller rotating at 120 rpm for 20 min. After degassing the hydrogen level is measured with an ABB AlSCAN unit. The hydrogen level in the degassed molten aluminum is in all cases less than 0.100 ml H_2/100 g of aluminum.

Fig. 1 shows a schematic diagram of the electromagnetic stirring workstation (ESW). The ESW consists of a stator of an electric motor adapted to operate in high temperature conditions. Under the ES conditions, the molten or semi-solid sample takes the place of the rotor. A W20 G3M Variac was used to supply the current under controlled conditions. Table 2 shows the electrical parameters and operation conditions of the ESW.

Following to the hydrogen measurements the 319 melt is poured into a 300 cm^3 (60 mm diameter and 100 mm in length) stainless steel-ceramic coated crucible. In the present paper the untreated sample (solidified in as cast conditions) is identified as reference sample. All test samples (reference and ES treated) are solidified inside the ESW. The ES treatments are conducted varying the AC current supplied to the electric motor from 2 to 8 A. Three samples per current intensity are cast and characterized. The results presented in this paper represent the average of the three samples. For all test samples the ES treatment started in the liquid state and ended in the semi-solid state. Both ends of the crucible (top and bottom) are insulated to minimize heat loss in the vertical direction and to promote the heat released in the radial direction [12]. All samples are allowed to solidify under natural heat exchange conditions, it means close to equilibrium conditions. All ES treatments are performed between 645 and 560 °C (~45 °C above liquidus and ~40 °C below liquidus).

Thermal analysis of the solidification process is carried out using the aluminum thermal analysis platform (AlTAP) [12–14,16,20]. AlTAP is a high resolution technique developed by the Light Metal Casting Group at the University of Windsor for analysis and melt characterization. The temperature vs. time history curve (cooling curve) and its respective first derivative curve are used to identify the 319 alloy metallurgical reactions and to characterize some of their features. The temperature range for the ES treatment has been selected based from the thermal analysis information collected from the reference samples. The cooling curve analysis is conducted using the Newtonian algorithm following the procedure presented in Ref. [12]. The apparent fraction solid (af_s) was determined to investigate the effect of ES treatment on Cu-rich phases.

The specimens for image analysis (dimensions of 50 mm × 75 mm × 8 mm) are extracted from all samples in close vicinity to the thermocouple (centre of the test sample). All samples are monitored using a K-type thermocouple located at the center of the sample. Following the pouring of the liquid metal into the crucible a thermocouple is placed at the center of the sample and is kept in the same position through and after the completion of the ES treatment. The thermal history data of each sample is collected until the sample reaches a temperature of 300 °C. For metallography the specimens are prepared following standard metallographic procedures. The scanning electron microscope (SEM) and grain size observations are conducted on deep etched specimens with the aim to reveal the morphology of Si present in the eutectic, secondary phases and the grain boundaries. SEM observations are made using a JEOL JSM 5800 microscope in the secondary electron (SE) mode operated at 15 kV. The etching operation is carried out for 90 s at room temperature using a 4%HF-destilated water solution.

Image analysis is conducted on a Leica system (Q550IW) equipped with an automated optical microscope and its associated software (QWin). Fifty analytical fields at 200× magnification are analyzed based on stereological characteristics such as area, aspect ratio and perimeter for Al–Si eutectic particles. The level of modification of Si was determined using the image analysis results and statistical procedures. The average secondary dendrite arm spacing (SDAS) is determined based on measurements of 50 randomly selected dendrites or cells for the respective reference or ES treated samples. The average grain size is determined following the procedures indicated in the E112-96^{E1} ASTM standard [18] using a section of 3 cm^2.

3. Results and discussions

The metallographic observations of the reference sample showed a microstructure comparable to a sand cast product and in the present paper is referred as unmodified microstructure. The main constituents of the unmodified microstructure are aluminum matrix, Al–Si eutectic, Al–Cu eutectic and Fe-rich phases (Fig. 2a). The Cu-rich phases were previously identified by Djurdjevic et al. [13] as blocky, eutectic and fine eutectic; for simplicity in the present paper these three phases will be referred as Cu-rich phases. In Figs. 2a and 3a are shown the phases present in the microstructure of the 319 as cast (ES untreated) alloy. The SEM was also used to qualitatively determine the chemical composition of the phases and to ensure their proper characterization (Fig. 3a). The results of the microstructure analysis indicates that the reference sample has an average SDAS of 73.8 ± 6.6 μm and a grain size (equivalent diameter) of 5.9 ± 0.7 mm. In Figs. 2a and 3a are presented the respective microstructures for the reference sample as observed by means of optical and scanning electron microscopy.

The micrographs of the ES treated sample using an AC current of 8 A are presented in Figs. 2b and 3b. The main characteristic that is observed in Fig. 2 for the reference and ES treated samples is the refinements of dendrites in the ES treated sample creating a semi-globular structure. This proves the efficiency of the ES treatment to minimize ameliorate dendrite. The phases that can be observed in the microstructure (Figs. 2b and 3b) of the ES treated sample using an intensity of 8 A are α-Al matrix, Al–Si eutectic, Fe-rich and Cu-rich phases.

In Fig. 4 are presented the following curves: cooling curve, first derivative and the base line for the respective reference and ES treated samples. The cooling curve is recorded during the solidification of the sample using AlTAP. The first derivative and baseline are determined using the Newtonian method following the procedures presented in Ref. [12]. Each change in slope represents a solidification reaction. For a pure element solidifying under equilibrium conditions a phase transformation reaction occurs isothermally and for a multi-component alloy occurs in a range of temperatures, which is the case for the alloys investigated herein. Unfortunately, in some cases the changes in slope for some reactions (e.g. Cu-rich phases) is not clear, compare Fig. 4a and b. Therefore, the determination of the first derivative is of interest since this curve clearly enhances the changes in slope of the cooling curve.

Each peak on the first derivative can be understood as a nucleation, growth and coarsening process for a solidification reaction. Hence, a change in these characteristics is directly translated in

Table 2
Electrical characteristics of the ES workstation.

Device	Phases	Current	AC voltage range (V)	Frequency (Hz)	Power factor	Rotation speed (rpm)
Stator	3	AC	230YY/460Y	60	0.7	1000
Variac	3	AC	230		N/A	N/A

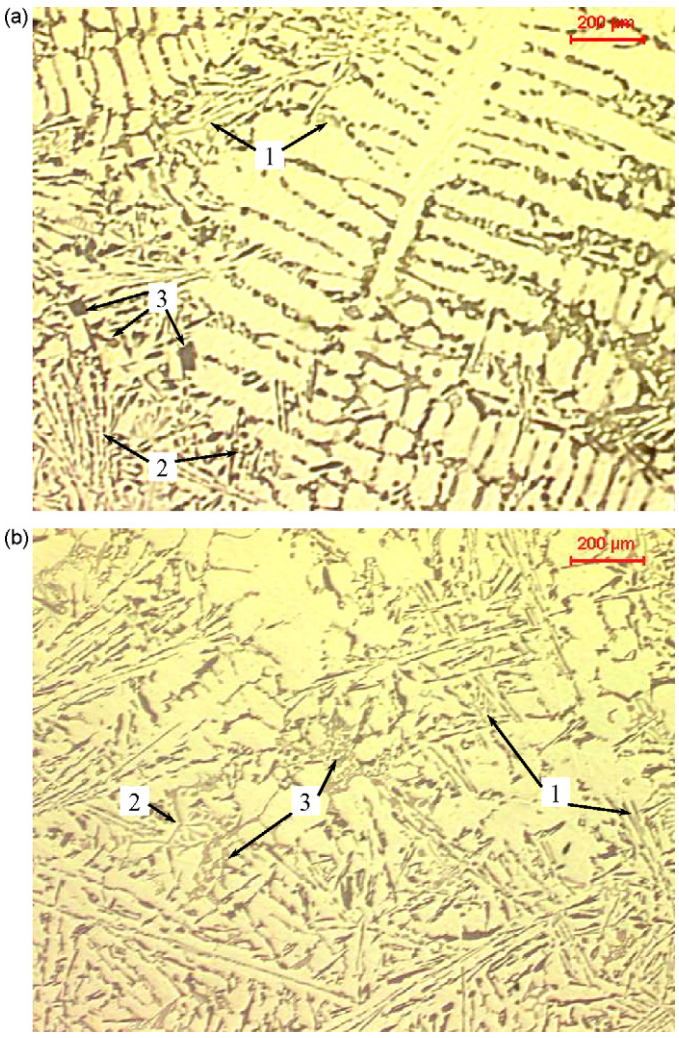

Fig. 2. Microstructure (50×) of the 319 alloy in (a) as-cast (reference) and (b) ES treated using an AC current of 8 A conditions. Both samples were solidified at a cooling rate of 0.12 °C/s. Numbers 1, 2 and 3 indicate the Al–Si, Fe base and Cu-rich phases.

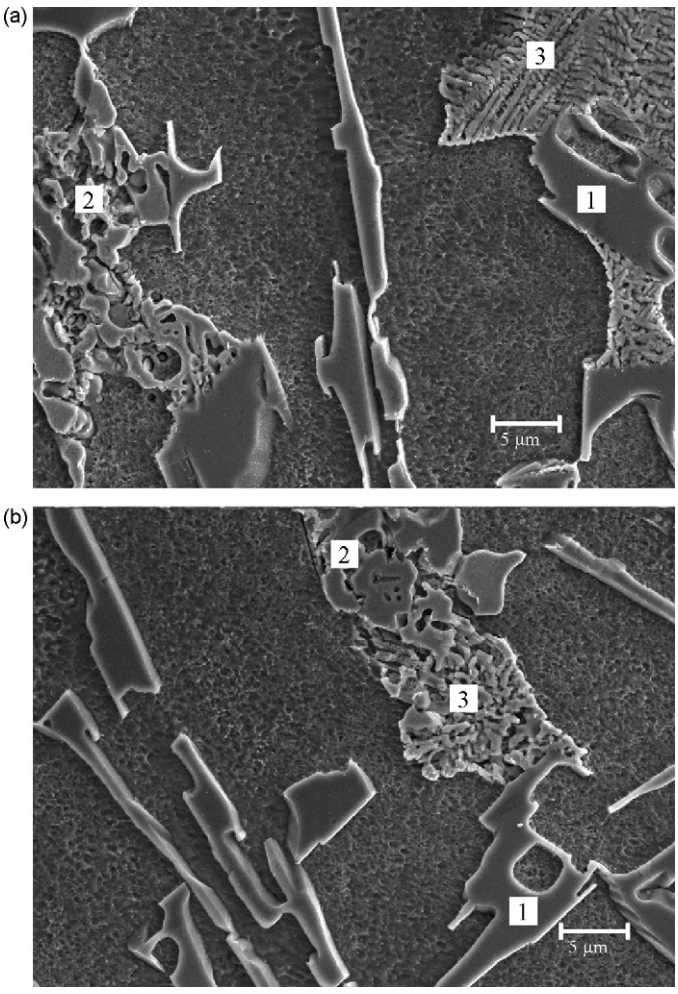

Fig. 3. SEM/SE micrographs (1000×) of the deep etched 319 alloy samples solidified at cooling rate of 0.12 °C/s: (a) reference and (b) ES treated using an AC current of 8 A. Note the various morphologies for the different Cu-rich phases in the reference sample. Numbers 1, 2 and 3 indicate the Al–Si, Fe base and Cu-rich phases.

a modification of the respective microstructure constituent. The area between the first derivative and the baseline (full integral) is an amount that is proportional to the heat released during the solidification of a sample. For the same phase the respective integral is proportional to the amount of exothermic heat (enthalpy of formation "ΔH_f") released during the nucleation and growth of such phase. Consequently, it can be said that the integral of two or more samples of the same composition that are solidified under same conditions must be the same. On the contrary, any change in the heat released during solidification or the calculated integral can be directly related to a microstructural change. Furthermore, when the integral is determined for a particular reaction the procedure is known as partial integral that allows a qualitative analysis of independent phases (e.g. Cu-rich). This allows quantifying any effect on microstructure due to ES or chemical means by thermal analysis.

Fig. 4a shows the thermal analysis results for the reference sample and is used to identify the phases that precipitate during solidification allowing a thermal characterization of the microstructure constituents (Figs. 2a and 3a). The solidification reactions identified by thermal analysis are: α-Al nucleation (601.8 ± 0.8 °C), Al–Si eutectic (568.9 ± 0.9 °C), Cu-rich phases (505.3 ± 1.3 °C). The solidification range for the reference sample is 122 ± 1.2 °C and the solidus temperature of the reference sample is 479.8 ± 1.1 °C. All samples solidified at an approximate cooling rate of 0.12 °C/s. The liquidus temperature for the reference sample is in agreement with the calculated liquidus temperature determined using the silicon equivalent (Si_{EQ}) algorithm [19].

Table 3
Characteristic temperatures for the metallurgical reactions and thermal analysis results for the reference and ES treated samples. The average standard deviation for the measure temperatures for the three samples analyzed per ES treatment condition is less than 1 °C.

AC current (A)	Cooling rate (°C)	Liquidus (°C)	Dendrite rigidity point temperature	Liquidus undercooling (°C)	Apparent fraction solid (af_s, %)
0	0.12	601.8	NA	1.62	11.52
2	0.12	604.2	601.4	0.95	9.63
4	0.12	604.8	600.5	0.74	7.77
6	0.12	605.5	597.4	0.57	6.80
8	0.12	605.9	594.6	0.47	6.70

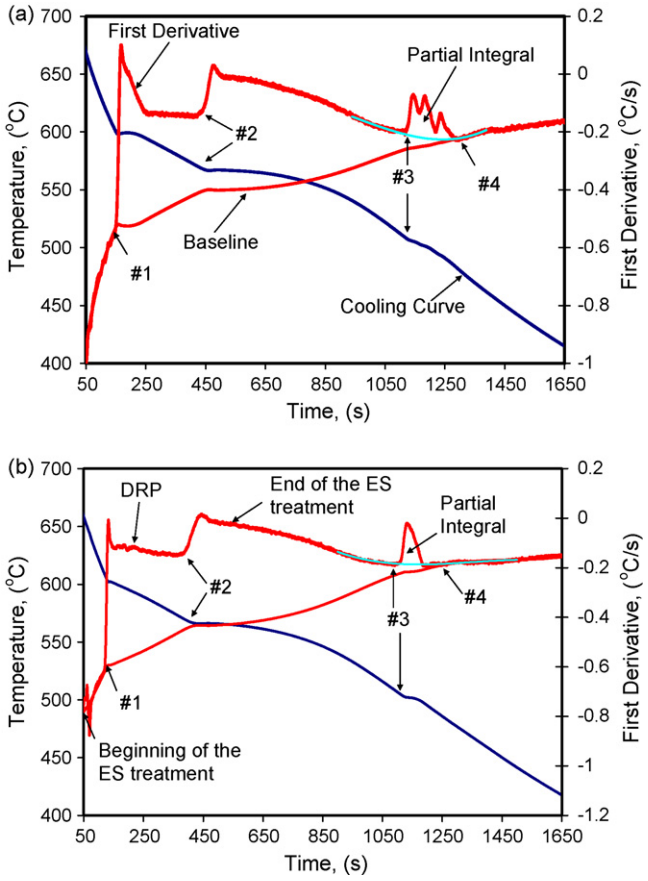

Fig. 4. Thermal analysis results obtained during the cooling cycle of the 319 alloy in (a) as-cast (reference) and (b) ES treated using an AC current of 8 A conditions. Note the differences in the reaction #3.

The partial integral is used to determine the effect of electromagnetic stirring on Cu-rich phases. Fig. 4 sketches the partial integral procedure that is also reported in Ref. [21]. The partial integral is calculated to determine the apparent fraction solid (af_s) that is proportional to the amount of precipitating phase for a particular reaction. The results of the apparent fraction solid are presented in Table 3. The apparent fraction solid results show a relationship among the intensity of the AC current used for the ES treatment and the level of modification of the Cu-rich phases. The partial integral method is simple and can be implemented for on-line screening of Al–Si alloys.

The electromagnetic field induced in the sample during the ES treatment creates a vortex; the intensity of the vortex is proportional to the applied AC current. The vortex's motion behaves as a blender breaking the early forming dendrites and increasing the number of nucleation sites resulting in an effective microstructure refining mechanism. The reduction in temperature and fraction solid increases for the ES treated samples result in an increase in the rigidity of the molten alloy and promotes a sudden stop (freezing) of the molten alloy. The temperature at which the vortex freezes is a function of the AC current intensity for the respective ES treatment.

The freezing temperature is identified as the dendrite rigidity point (DRP). The DRP temperature for the ES treated samples change from 601.3 to 594.6 °C for the corresponding ES treated samples using 2 and 8 A. Under the investigated conditions it is noticed that the freezing temperature decreases as the ES treatment intensity increases that is due to a higher torque induced by the respective current. By increasing the induced torque forces it is possible to break the solidifying dendrites in the presence of larger amounts of fraction solid (lower temperatures) preventing the excessive formation of dendrites. Therefore, the analysis of the DRP temperature can lead to the determination of the level of modification of the α-Al matrix. Detailed information regarding the DRP temperatures is given in Table 3.

Fig. 4b shows a representative cooling curve for the ES treated sample using an AC current of 8 A and the following solidification reactions and their respective nucleation temperature are identified: α-Al nucleation temperature (T_{LIQ} 605.9 ± 0.5 °C), Al–Si eutectic ($T_{E,NUC}{}^{Al-Si}$ 569.6 ± 0.5 °C), and nucleation the Cu-rich phase ($T_{E,NUC}{}^{Cu}$ = 506.6 ± 0.8 °C). Fig. 4b shows that the metallurgical reactions appear at comparable temperatures as in the reference sample. It is important to mention that the identification of the Fe-rich phase(s) in the cooling curves is challenging for the following two reasons: (i) the limited amount of Fe present in the alloy and (ii) Fe phase(s) precipitates together with the α-Al, it means both peaks are convoluted.

The grain size measurements show that the ES treatment can reduce the grain size approximately 6 times (from 5.9 to 1 mm) and the number of grain per square centimeter increased more than 30 times (from 2.9 to 93.5 grains/cm^2). The ES treated sample using an AC = 8 A show a dendritic cells refinement of approximately 12% when compared to the reference sample. Table 4 summarizes the above mentioned microstructure analysis results.

Point #3 in Fig. 4a and b corresponds to the Cu-rich phases and it is evident that in both cases the number of peaks, hence Cu-rich solidification reactions, is different. For instance, the fine eutectic (third peak) is not present in the cooling curve for the ES treated sample using a current of 8 A. In fact, the intensity of this peak reduces gradually as the AC current increases (Fig. 5). This is most likely due to a potential dissolution of Cu present in the fine eutectic phase in the aluminum matrix. This is an indication that the ES treatment enhanced the solubility of Cu into the Al matrix or inhibits the formation and precipitation of the Cu fine eutectic. The analysis of the apparent fraction solid (Table 3) can lead to determine the effect of the ES treatment on Cu-rich phases. The reduction in the apparent fraction solid of Cu is further confirmed with the results of metallography presented in Fig. 3.

As a result of the microstructure refinement presented by the ES treated samples it is observed a significant increase in the number of grains, it means the grain is refined. The grain refinement results are presented in Table 4 and show a good agreement with the AC current used for the ES treatments. In addition, the reduction of the Cu fine eutectic phase in the microstructure of the ES treated samples is more evident as the current used for the ES treatment

Table 4
Relationships between ES conditions (AC current) and microstructure characteristics for the reference and ES treated samples for the 319 alloy.

AC current (A)	Grain size (Ø mm)	Confidence		Dendrite arm/cell spacing (μm)	Confidence	
		95%	99%		95%	99%
0	5.9 ± 0.7	0.2	0.27	73.85 ± 6.6	1.9	2.5
2	2.9 ± 0.3	0.09	0.11	72.20 ± 6.4	1.8	2.4
4	2.1 ± 0.5	0.14	0.19	71.51 ± 4.3	1.2	1.6
6	1.6 ± 0.2	0.06	0.08	67.34 ± 5.7	1.7	2.2
8	1.0 ± 0.07	0.02	0.03	66.36 ± 5.7	1.7	2.2

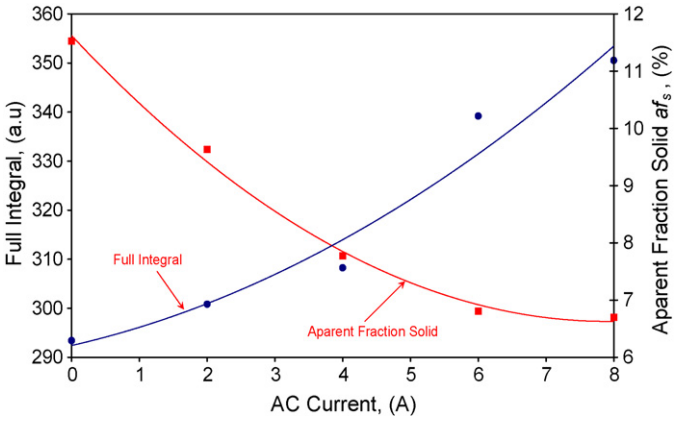

Fig. 5. Apparent fraction solid (af_s in %) indicating the reduction of the Cu-rich phases by the effect of the electromagnetic stirring treatment.

increases. This is an expected effect, but what is important is the good correlation with thermal analysis results (Fig. 4).

Liquidus temperature is of interest since it changes as a function of the current used for the ES treatments. In fact, this is a well-known effect and has been reported in the literature for melts refined by chemical means [15–17]. Therefore, a correlation among the effect of ES on grain size and the liquidus temperature can be established. Unfortunately, the change in liquidus temperature occurs in a narrow range, which may compromise its accuracy when used to determine grain refinement. In addition, liquidus temperature is a function of composition; for example, 1 wt% Si can alter the liquidus temperature of Al–Si hypo and hypereutectic alloys in 18.9 °C or more. Conversely, the undercooling seems observed in the liquidus solidification reaction seems to be more promising methodology for grain size determination. This is because undercooling is almost independent of chemical composition and is more dependable of the solidification conditions, hence level of refinement. Fig. 6 sketches the analysis of the undercooling of the liquidus temperature.

In Fig. 7 is presented the results of the analysis of the undercooling of the α-Al nucleation reaction, which is in agreement with the refinement of the microstructure. This correlation makes the use of thermal analysis attractive for on-line determination of grain refinement on ES treated Al–Si alloys and potentially for chemically modified alloys too.

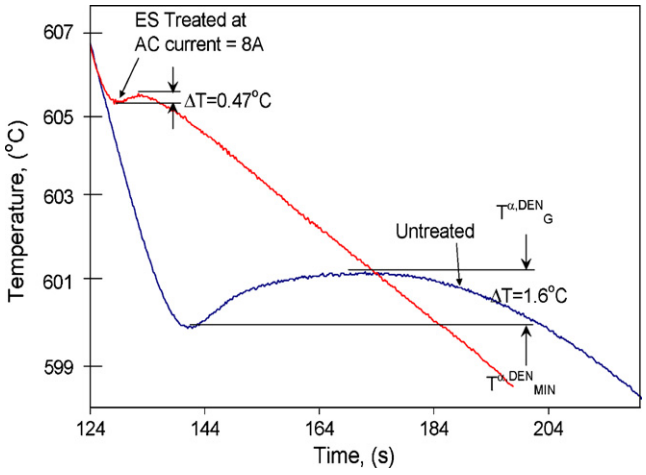

Fig. 6. Segment of the temperature vs. time cooling curve showing the differences in liquidus undercooling and the difference in liquidus temperatures for the reference and ES treated sample using an AC current of 8 A.

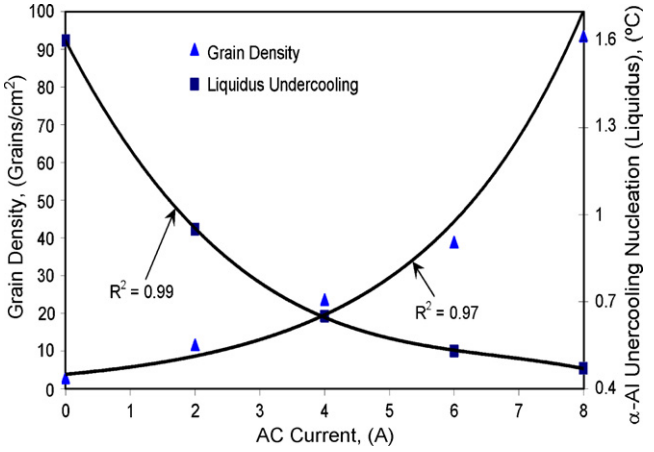

Fig. 7. Effect of ES treatment conditions (AC current) on grain size and undercooling for the α-Al nucleation reaction on the 319 alloy.

In following is presented a series of equations that are developed for an on-line screening method to predict the characteristics of the microsctructure. The characteristics that can be predicted are: dendrite arm spacing (Eq. (1)), grain size (Eq. (2)), liquidus undercooling temperature (Eq. (3)), full integral (Eq. (4)) and apparent fraction solid "af_s" (Eq. (5)). All equations were determined as a function of the AC current used during the ES treatment. It is important to mention that the mathematical models presented herein are applicable for the conditions and alloy investigated in this research. Nonetheless, the approach is presented for its simplicity and to show its potential for industrial or research implementation:

$$DAS = -0.99(AC_{Current}) + 74.21, \quad R^2 = 0.94 \tag{1}$$

$$GS = 5.25\exp^{(-0.21\times AC_{Current})}, \quad R^2 = 0.97 \tag{2}$$

$$\Delta T = 0.023(AC_{Current})^2 - 0.316(AC_{Current}) + 1.567, \quad R^2 = 0.99 \tag{3}$$

$$Full.Integral = 0.5596(AC_{Current})^2 - 3.152(AC_{Current}) + 292.4, \quad R^2 = 0.95 \tag{4}$$

$$af_s = 0.08(AC_{Current})^2 - 1.26(AC_{Current}) + 11.62, \quad R^2 = 0.99 \tag{5}$$

where GS is the grain size (mm), DAS is the dendrite arm spacing (μm), ΔT is the liquidus undercooling (°C), $AC_{Current}$ is the AC current used for the ES treatment (A), and af_s is the apparent fraction solid (%).

4. Conclusions

Based on the experimental results it was found that the ES treatments performed on the 319 alloy in a semi-solid state had an effect on the microstructure modification. The metallographic observations of the ES treated samples showed a microstructure transition from dendritic to quasi-cellular as a function of the ES treatment conditions. Higher AC currents are associated with higher microstructure refinement, more globular microstructure and the reduction of the Cu eutectic. The average grain size in the ES treated sample using 8 A is approximately six times smaller (~1 mm in diameter) than in the reference sample (~5.9 mm in diameter). The precipitation of the Cu present in the Al–Cu fine eutectic can be inhibited by the ES treatment that is observed by microscopy means and further confirmed with thermal analysis (apparent fraction solid "af_s"). The Si present in the Al–Si eutectic does not seem to be affected by the ES treatment.

Based on the results from image analysis and thermal analysis from untreated and ES treated samples, the level of microstructure

modification is in statistically agreement with the thermal analysis results. This opens the opportunity to propose an on-line quality control algorithm to predict the effects of microstructure modification and grain refinement for the 319 Al–Si alloy solidified under the investigated conditions.

Acknowledgements

FCRH would like to acknowledge CONACyT-Mexico for the invaluable support towards his PhD studies. Both authors would like to express their appreciation to the Natural Sciences and Engineering Council of Canada (NSERC).

References

[1] A.T. Spada, Eng. Cast. Solutions 4 (2002) 28–31.
[2] S. Chul-Lim, E.-P. Yoon, J. Mater. Sci. Lett. 16 (1997) 104–109.
[3] A. Voguel, R.D. Doherty, B. Candtor, Metall. Sci. 1 (1979) 518.
[4] R.T. Southin, J. Inst. Met. 94 (1966) 401.
[5] C. Vives, Met. Mater. Trans. B 27B (1996) 457–464.
[6] C. Vives, Met. Mater. Trans. B 27B (1996) 465.
[7] M.C. Flemings, Met. Mater. Trans. B 22 (1999) 269–293.
[8] Y.S. Yang, C.Y.A. Tsao, Viscosity and Structure Variations of Al–Si Alloys in the Semi-Solid State, Cheapman and Hall, 1997, pp. 2087–2092.
[9] V. Abramov, O. Abramov, V. Bulgakov, F. Sommer, J. Mater. Lett. 37 (1998) 27–34.
[10] G. Horan, M. Jiaji, B. Xoufang, Trans. Non-Ferrous Met. Soc. 7 (1997) 137–141.
[11] S.C. Bersagma, M.C. Tolle, M.E. Kassner, X. Li, E. Evangelista, Mater. Sci. Eng. A 237 (1997) 24–34.
[12] W.T. Kierkus, J.H. Sokolowski, AFS Trans. 107 (1999) 161–167.
[13] M.B. Djurdjevic, W. Kasprzak, C.A. Kierkus, W.T. Kierkus, J.H. Sokolowski, AFS Trans. (2001) 517–528.
[14] J. Chen, M. Kasprzak, W. Kasprzak, J.H. Sokolowski, 15th International Congress and Expo of the Foundry Industry, Monterrey Mexico, October 2–4, 2003, pp. 147–158.
[15] H. Jiang, J.H. Sokolowski, M. Djurdjevic, W. Evans, AFS Trans. 22 (2000) 505–510.
[16] R. MacKay, M. Djurdjevic, H. Jiang, J.H. Sokolowski, W. Evans, AFS Trans. 24 (2000) 511–520.
[17] M.B. Djurdjevic, J.H. Sokolowski, T.J. Stockwell, J. Metall. 4 (1998) 237–248.
[18] ASTM International, E112-96^{E1}, 03.01, 1996, pp. 251–274.
[19] F.C. Robles Hernández, M.B. Djurdjevic, W.T. Kierkus, J.H. Sokolowski, Mater. Sci. Eng. A 396 (2005) 271–276.
[20] M.B. Djurdjevic, W.T. Kierkus, J.H. Sokolowski, Cast Components and Their Processes, University of Windsor, Brochure 29, 2004.
[21] F.C. Robles Hernández, J.H. Sokolowski, J. Alloys Compd. 419 (2005) 180–190.